J Toxicol Pathol 2018; 31: 169–178

Original Article

Role of oxidative stress in the chemical structure-related genotoxicity of nitrofurantoin in *Nrf2*-deficient *gpt* delta mice

Takuma Tsuchiya[1, 2], Aki Kijima[1], Yuji Ishii[1], Shinji Takasu[1], Yuh Yokoo[1], Akiyoshi Nishikawa[1], Tokuma Yanai[2], and Takashi Umemura[1, 3*]

[1] Division of Pathology, National Institute of Health Sciences, 3-25-26 Tonomachi, Kawasaki-ku, Kawasaki-shi, Kanagawa 210-9501, Japan
[2] Pathogenetic Veterinary Science, United Graduate School of Veterinary Sciences, Gifu University, 1-1 Yanagido, Gifu-shi, Gifu 501-1193, Japan
[3] Department of Animal Nursing, Yamazaki Gakuen University, 4-7-2 Minamiosawa, Hachioji-shi, Tokyo 192-0364, Japan

Abstract: Despite its antimicrobial activity, nitrofurantoin (NFT) is a renal carcinogen in rats. Oxidative stress induced by reduction of the nitro group of NFT may contribute to its genotoxicity. This is supported by our recent results indicating that the structure of the nitrofuran plays a key role in NFT-induced genotoxicity, and oxidative DNA damage is involved in renal carcinogenesis. Nuclear factor erythroid 2-related factor 2 (NRF2) regulates cellular responses to oxidative stress. To clarify the role of oxidative stress in the chemical structure-related genotoxic mechanism of NFT, we performed reporter gene mutation assays for NFT and 5-nitro-2-furaldehyde (NFA) using *Nrf2*-proficient and *Nrf2*-deficient *gpt* delta mice. NFT administration for 13 weeks resulted in a significant increase in 8-hydroxydeoxyguanosine (8-OHdG; a marker of oxidative stress) and *gpt* mutant frequency only in the kidneys of *Nrf2*$^{-/-}$ mice. The mutation spectrum, characterized by increased substitutions at guanine bases, suggested that oxidative stress is involved in NFT-induced genotoxicity. However, NFA did not increase the mutation frequency in the kidneys, despite the increased 8-OHdG in NFA-treated *Nrf2*$^{-/-}$ mice. Thus, it is unlikely that oxidative stress is involved in the genotoxic mechanism of NFA. These results imply that nitro reduction plays a key role in the genotoxicity of NFT, but the lack of a role of oxidative stress in the genotoxicity of NFA indicates a potential role of side chain interactions in oxidative stress caused by nitro reduction. These findings provide a basis for the development of safe nitrofurans. (DOI: 10.1293/tox.2018-0014; J Toxicol Pathol 2018; 31: 169–178)

Key words: nitrofurantoin, NRF2, oxidative stress, *in vivo* mutagenicity, kidney

Introduction

Nitrofurans are antimicrobial compounds that contain a nitro group at the 5-position of the furan ring and an amine or hydrazide side chain derivative (Fig. 1). Some nitrofurans are prohibited from use in veterinary medicine in Japan owing to their genotoxic and carcinogenic potential[1–4]. However, new nitrofurans with various hydrazide derivatives on the side chain are being developed, given their easy synthesis and high antimicrobial activity[5, 6]. Therefore, it is necessary to clarify the chemical structure-related genotoxicity of nitrofurans to facilitate risk assessments for human applications.

Received: 10 March 2018, Accepted: 26 April 2018
Published online in J-STAGE: 2 June 2018
*Corresponding author: T Umemura (e-mail: umemura@nihs.go.jp)
©2018 The Japanese Society of Toxicologic Pathology
This is an open-access article distributed under the terms of the Creative Commons Attribution Non-Commercial No Derivatives (by-nc-nd) License. (CC-BY-NC-ND 4.0: https://creativecommons.org/licenses/by-nc-nd/4.0/).

One nitrofuran group, nitrofurantoin (NFT), is synthesized by the condensation of 5-nitro-2-furaldehyde (NFA) (Fig. 1) and 1-aminohydantoin and is a renal carcinogen in rats[7]. The formation of reactive oxygen species (ROS) or intermediates resulting from the reduction of the nitro group of NFT is thought to exert antibacterial activity[8–10]. Accordingly, we hypothesized that oxidative stress is involved in NFT-induced renal carcinogenesis. We recently demonstrated significant increases in the levels of 8-hydroxydeoxyguanosine (8-OHdG), an oxidized DNA lesion, and *gpt* mutant frequencies (MFs) with substitutions at guanine bases in the kidneys of *gpt* delta rats treated with NFT[11]. However, the 1-aminohydantoin side chain did not increase 8-OHdG levels or *gpt* MFs[11]. NFA containing a nitro group, similar to NFT, did not increase 8-OHdG levels but increased *gpt* MFs in the kidneys of *gpt* delta rats with different mutation spectra from those for NFT[11]. Accordingly, the relationship between NFT-induced oxidative stress and its chemical structure remains unclear[11].

The redox-sensitive transcription factor nuclear factor erythroid 2-related factor 2 (NRF2) regulates cellular responses to oxidative stress. NRF2 is anchored in the cy-

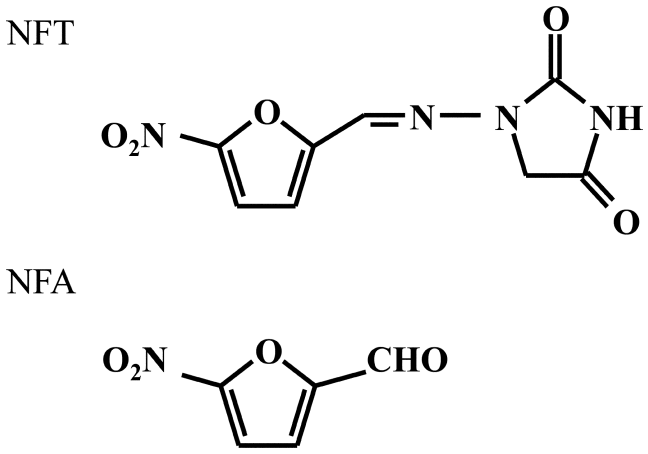

Fig. 1. Chemical structures of NFT and NFA.

toplasm by Kelch-like ECH-associated protein 1 (KEAP1), which also mediates the proteasomal degradation of NRF2. Oxidative stress causes the dissociation of NRF2 from KEAP1 and leads to NRF2 translocation into the nucleus, where it can bind to the antioxidant response element (ARE) and consequently transactivate ARE-bearing genes encoding antioxidant-related enzymes, such as NAD(P)H:quinone oxidoreductase 1 (NQO1), heme oxygenase 1 (HO1), and glutathione *S*-transferase[12, 13]. Thus, the NRF2-ARE pathway has broad protective effects against oxidative stress. *Nrf2*-deficient mice clearly show greater sensitivity to various toxicants, as evidenced by induction of the oxidative stress response following exposure to acetaminophen, 4-vinylcyclohexene diepoxide, pentachlorophenol, 2-amino-3-methylimidazo[4,5-f]quinoline, ferric nitrilotriacetate, and piperonylbutoxide[14–20].

In the present study, the role of oxidative stress in the chemical structure-related genotoxicity of NFT was determined using *Nrf2*-proficient and *Nrf2*-deficient mice exposed to NFT or NFA for 13 weeks, followed by reporter gene mutation assays[21, 22] and measurements of 8-OHdG levels in the kidney.

Materials and Methods

Chemicals

NFT ($C_8H_6N_4O_5$, MW 238.2, CAS No. 67-20-9) and NFA ($C_5H_3NO_4$, MW 141.08, CAS No. 698-63-5) were purchased from Sigma-Aldrich Corporation (St. Louis, MO, USA) and were suspended in 0.5 w/v% methyl cellulose 400 cP solution (Wako Pure Chemical Industries, Ltd., Osaka, Japan). Suspensions of the test chemicals were used at a volume of 10 mL/kg body weight (BW), based on BW on the day of chemical administration to *Nrf2*$^{+/+}$ or *Nrf2*$^{-/-}$ *gpt* delta mice.

Animals, diet, and housing conditions

The study protocol was approved by the Animal Care and Utilization Committee of the National Institute of Health Sciences. *Nrf2*-deficient mice with the C57BL/6J background established by Itoh *et al.*[23] were crossed with *gpt* delta mice with the C57BL/6J background (Japan SLC, Shizuoka, Japan). *Nrf2*$^{-/-}$ *gpt* delta mice and *Nrf2*$^{+/+}$ *gpt* delta mice were then obtained from the F1 generation and genotyped by polymerase chain reaction (PCR) with DNA collected from the tail of each mouse. All mice were housed in polycarbonate cages (5 mice per cage) with hard wood chips for bedding in a conventional animal facility maintained at a controlled temperature (23 ± 2°C) and humidity (55 ± 5%), with 12 air changes per hour and a 12-h light/dark cycle. Mice were given free access to a basal diet (CRF-1, Charles River Laboratories Japan, Kanagawa, Japan) and tap water.

Experimental design

Eight-week-old male mice of each genotype were divided into five groups (four or five mice per group), i.e., two groups each administered NFT or NFA by gavage for five consecutive days and a control group administered vehicle alone, and the total administration period was 13 weeks. For daily doses, 70 and 35 mg/kg NFT were used. The maximum tolerated dose of NFT was 70 mg/kg in a preliminary dose selection study. No remarkable changes were observed in the general condition of mice treated with NFT at a dose of 70 mg/kg in the preliminary study. The daily doses of NFA were set to 41 and 21 mg/kg, the same molar doses used for NFT. BW was measured every week. At the end of administration for 13 weeks, animals were euthanized by exsanguination under isoflurane (Mylan Inc., Tokyo, Japan) anesthesia, and the bilateral kidneys were collected and weighed. A portion of the kidney tissues was frozen with liquid nitrogen and stored at −80°C for an *in vivo* mutation assay, 8-OHdG measurements, and western blotting. Another portion of the collected kidney tissues was homogenized in ISOGEN (Nippon Gene, Tokyo, Japan) and stored at −80°C until use for the isolation of total RNA.

In vivo mutation assays

6-Thioguanine (6-TG) and Spi$^-$ selection were performed using the methods described by Nohmi, *et al*[21]. Briefly, genomic DNA was extracted from the kidneys of animals in each group using a RecoverEase DNA Isolation Kit (Agilent Technologies, Santa Clara, CA, USA), and lambda EG10 DNA (48 kb) was rescued as phages by *in vitro* packaging using Transpack Packaging Extract (Agilent Technologies). For 6-TG selection, packaged phages were incubated with *Escherichia coli* YG6020, which expresses Cre recombinase, and converted to plasmids carrying *gpt* and chloramphenicol acetyltransferase genes. Infected cells were mixed with molten soft agar and poured onto agar plates containing chloramphenicol and 6-TG. To determine the total number of rescued plasmids, infected cells were

also poured on plates containing chloramphenicol without 6-TG. The plates were then incubated at 37°C for selection of 6-TG-resistant colonies, and the *gpt* MF was calculated by dividing the number of *gpt* mutants after clonal correction by the number of rescued phages. The *gpt* mutations were characterized by the amplification of a 739-bp DNA fragment containing the 456-bp coding region of the *gpt* gene[21] and sequencing the PCR products using an Applied Biosystems 3730*xl* DNA Analyzer (Life Technologies Corporation, Carlsbad, CA, USA). For Spi$^-$ selection, packaged phages were incubated with *E. coli* XL-1 Blue MRA for survival titration and *E. coli* XL-1 Blue MRA P2 for mutant selection. Infected cells were mixed with molten lambda-trypticase agar plates. The next day, plaques (Spi$^-$ candidates) were punched out with sterilized glass pipettes, and the agar plugs were suspended in SM buffer. The Spi$^-$ phenotype was confirmed by spotting the suspensions on three types of plates where the XL-1 Blue MRA, XL-1 Blue MRA P2, or WL95 P2 strain was spread on soft agar. Spi$^-$ mutants forming clear plaques were counted on every plate.

Measurement of 8-OHdG

Renal DNA of *Nrf2*$^{-/-}$ *gpt* delta mice and *Nrf2*$^{+/+}$ *gpt* delta mice was extracted and digested as described previously[24]. Briefly, nuclear DNA was extracted using a DNA Extractor WB Kit (Wako Pure Chemical Industries). To prevent artefactual oxidation in the cell lysis step, deferoxamine mesylate (Sigma-Aldrich) was added to the lysis buffer. DNA was digested to deoxynucleotides by treatment with nuclease P1 and alkaline phosphatase using an 8-OHdG Assay Preparation Reagent Kit (Wako Pure Chemical Industries). The levels of 8-OHdG (8-OHdG/10^5dG) were measured for three randomly selected mice in each group by high-performance liquid chromatography using an electrochemical detection system (Coulochem II, ESA, Bedford, MA, USA) as previously reported[25]. Because of the quite small amount of kidney samples applied for measurement, the data were obtained from only one mouse in the 41 mg/kg NFA group.

RNA isolation and quantitative real-time PCR for mRNA expression

Total RNA was extracted using ISOGEN according to the manufacturer's instructions. cDNA copies of total RNA were obtained using a High-Capacity cDNA Reverse Transcription Kit (Life Technologies).

All PCRs were performed using an Applied Biosystems 7900HT FAST Real-Time PCR System with primers for mouse *Nqo1* obtained from TaqMan® Gene Expression Assays and TaqMan® Rodent GAPDH Control Reagents. Expression levels were calculated by the relative standard curve method and were determined relative to *Gapdh* levels. Data are presented as fold-change values of treated samples relative to controls.

Protein extraction, SDS-PAGE, and western blotting

The kidneys from all animals were homogenized using a Teflon homogenizer with ice-cold RIPA lysis buffer (Wako Pure Chemical Industries) containing mammalian protease inhibitor cocktail. Samples were homogenized and centrifuged at 15,000 × *g* for 30 min, and the resulting supernatants were used. Protein concentrations were determined using an Advanced Protein Assay (Cytoskeleton, Denver, CO, USA) with bovine serum albumin as a standard. Samples were separated by SDS-polyacrylamide gel electrophoresis (SDS-PAGE) and transferred to 0.45-μm PVDF membranes (Millipore, Billerica, MA, USA). For the detection of target proteins, membranes were incubated with an anti-NQO1 polyclonal antibody (1:1,000; Abcam, Cambridge, UK) and anti-β-actin monoclonal antibody (1:3,000; Abcam) at 4°C overnight. Secondary antibody incubation was performed using horseradish peroxidase-conjugated secondary anti-rabbit or anti-mouse antibody at room temperature. Protein detection was facilitated by chemiluminescence using ECL Plus (GE Healthcare Japan Ltd., Tokyo, Japan).

Statistical analysis

Data are presented as the mean ± standard deviation (SD). Statistical analyses of differences in BWs, kidney weights, 8-OHdG levels, mRNA expression levels, *gpt* and Spi$^-$ MFs, and *gpt*-mutation spectra relative to the values of the control group of mice of the same genotype were analyzed by Dunnett's multiple comparison test. Comparison between mRNA expression levels of each control group of *Nrf2*-proficient and *Nrf2*-deficient mice were made using Student's *t*-test. $P<0.05$ was considered significant.

Results

Body and kidney weights

Body and kidney weights of *Nrf2*-proficient and *Nrf2*-deficient mice treated with NFT or NFA for 13 weeks are summarized in Fig. 2 and Table 1. For both genotypes, there were no significant differences in body and kidney weights between treated and untreated mice.

Quantitative real-time PCR and western blotting analyses of Nqo1

For both genotypes, the mRNA expression level of *Nqo1* was not significantly influenced by NFT or NFA treatment. In *Nrf2*-deficient mice, however, the *Nqo1* mRNA expression level was significantly lower than that in *Nrf2*-proficient mice (Fig. 3).

Furthermore, at the protein expression level, NQO1 was not affected by NFT or NFA treatment. In *Nrf2*-deficient mice, however, the NQO1 protein expression level was lower than that in *Nrf2*-proficient mice (Fig. 3).

8-OHdG levels in kidney DNA

8-OHdG levels in *Nrf2*-deficient mice treated with 70 mg/kg NFT were significantly higher than those in control mice. 8-OHdG levels in *Nrf2*-deficient mice treated with

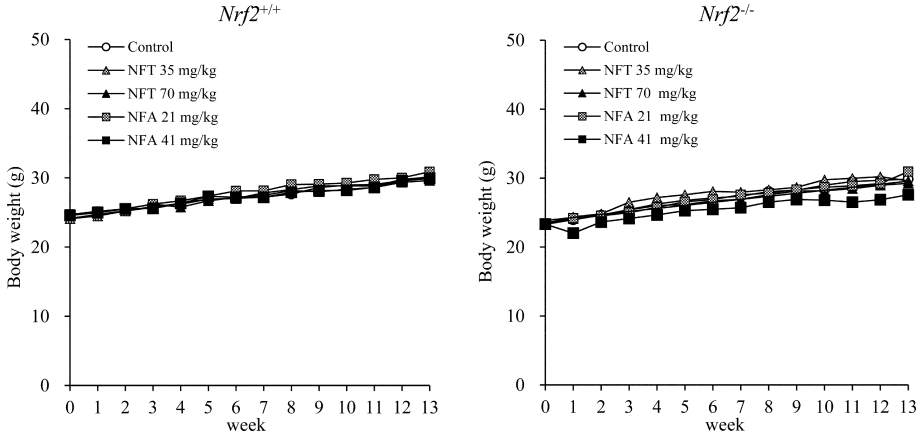

Fig. 2. Growth curves for *Nrf2*$^{+/+}$ (left panel) and *Nrf2*$^{-/-}$ (right panel) mice treated with NFT or NFA for 13 weeks. For both genotypes, there were no significant differences in body weight between treated and untreated mice.

Table 1. Final Body and Kidney Weights of Male *Nrf2*$^{+/+}$ or *Nrf2*$^{-/-}$ *gpt* Delta Mice Treated with NFT or NFA for 13 Weeks

		Control	NFT		NFA	
			35 mg/kg	70 mg/kg	21 mg/kg	41 mg/kg
Nrf2$^{+/+}$	No. of animals	5	5	5	5	5
	Final body weights (g)	30.05 ± 1.51[b]	30.14 ± 1.06	29.62 ± 2.09	30.88 ± 1.25	29.93 ± 2.49
	Kidneys (g)	0.39 ± 0.02	0.36 ± 0.01	0.37 ± 0.05	0.37 ± 0.03	0.37 ± 0.05
	Kidneys (g%)[a]	1.31 ± 0.07	1.20 ± 0.03	1.25 ± 0.11	1.19 ± 0.09	1.22 ± 0.11
Nrf2$^{-/-}$	No. of animals	5	5	4	5	5
	Final body weights (g)	29.86 ± 2.85	29.60 ± 3.58	29.26 ± 3.15	30.94 ± 2.80	27.59 ± 1.40
	Kidneys (g)	0.36 ± 0.04	0.36 ± 0.08	0.38 ± 0.06	0.36 ± 0.05	0.31 ± 0.05
	Kidneys (g%)[a]	1.20 ± 0.04	1.22 ± 0.17	1.28 ± 0.10	1.15 ± 0.07	1.13 ± 0.16

[a]Kidneys-to-body weight ratios (relative weights) are given as grams organ weight/grams body weight. [b]Mean ± SD.

NFA showed tendencies toward increasing in a dose-dependent manner, although they were not statistically significant because of insufficiency of samples in the 41 mg/kg NFA group. No increase was observed in *Nrf2*-proficient mice treated with NFT or NFA at any dose (Fig. 4).

In vivo mutation assay

Results of the *gpt* assay for the kidneys of *Nrf2*-proficient and *Nrf2*-deficient mice treated with NFT or NFA are shown in Tables 2 to 4. The *gpt* MFs in *Nrf2*-deficient mice treated with NFT at 70 mg/kg were significantly greater than those in the control group (Table 2). Increases in G-base substitutions including G:C to T:A or G:C to C:G transversions were observed in *Nrf2*-deficient mice treated with NFT, although there were no statistically significant differences (Table 4). The results of the Spi$^-$ assay are summarized in Table 5. There were no significant changes in Spi$^-$ MFs in *Nrf2*-proficient and *Nrf2*-deficient mice treated with NFT or NFA at any dose.

Discussion

Nrf2 plays a crucial role in protection against oxidative stress by transcriptionally upregulating various antioxidant enzymes, including NQO1[12, 13]. Previous studies have shown that *Nrf2*$^{-/-}$ mice show high sensitivity to various toxicants, including the induction of the oxidative stress response following exposure to acetaminophen, 4-vinylcyclohexene diepoxide, pentachlorophenol, 2-amino-3-methylimidazo[4,5-f]quinoline, ferric nitrilotriacetate, and piperonylbutoxide[14–20]. Although there were no dose-dependent effects in either genotype, the mRNA expression level of *Nqo1* in the kidneys of vehicle-treated *Nrf2*$^{-/-}$ mice was significantly lower than that of vehicle-treated *Nrf2*$^{+/+}$ mice, consistent with the results observed for the protein expression of NQO1. Thus, our results confirmed that *Nrf2*$^{-/-}$ mice are susceptible to oxidative stress. NFT administration for 13 weeks resulted in a significant increase in 8-OHdG in a dose-dependent manner only in the kidneys of *Nrf2*$^{-/-}$ mice. Administration of NFA also tended to result in a dose-dependent increase in 8-OHdG in *Nrf2*$^{-/-}$ mice. These results in the present study suggested that NFT and NFA induced oxidative stress in the kidneys of mice and that NFT might induce severer oxidative stress than NFA.

A significant increase in *gpt* MFs was observed in the kidneys of NFT-treated *Nrf2*$^{-/-}$ mice, but not in *Nrf2*$^{+/+}$ mice. In NFT-treated *Nrf2*$^{-/-}$ mice, the frequencies of specific mutations and, in particular, the rates of G:C to T:A and G:C

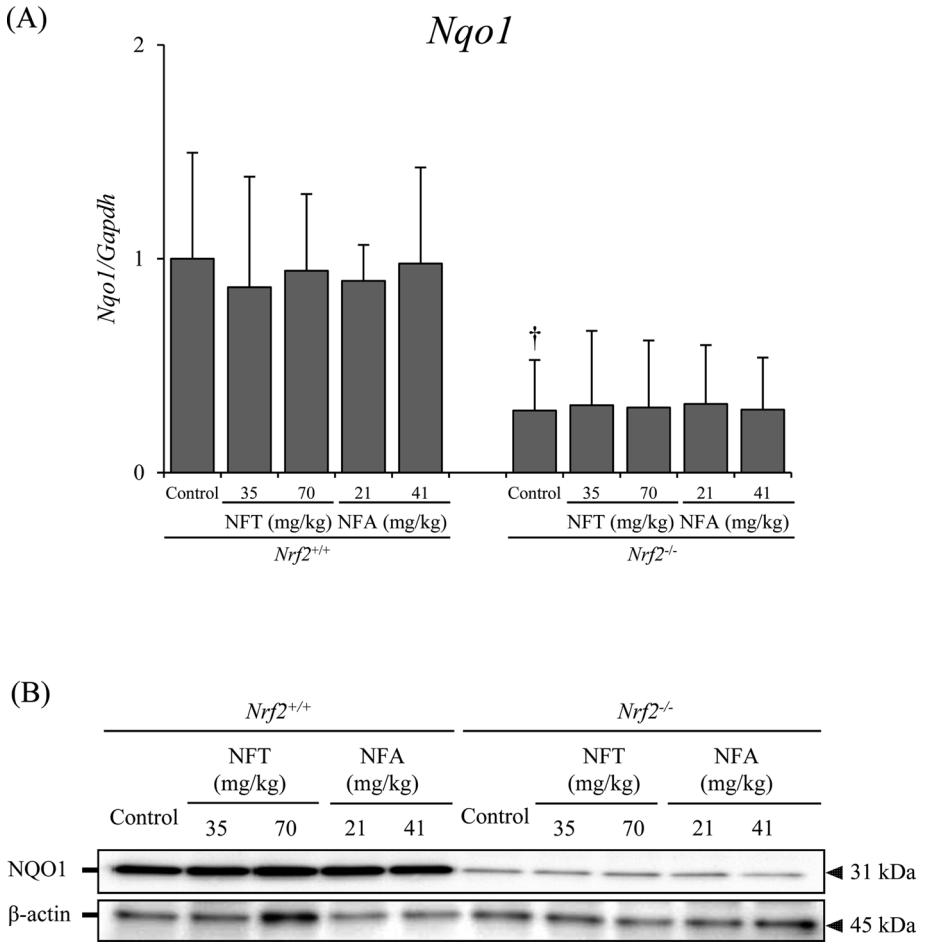

Fig. 3. Changes in the Nrf2-target gene *Nqo1* at the mRNA (A) and protein levels (B). (A) Data are presented as means ± SD. †mRNA expression levels in the *Nrf2*$^{-/-}$ control group were significantly different (P<0.05) from levels in the *Nrf2*$^{+/+}$ control group by Student's *t*-test.

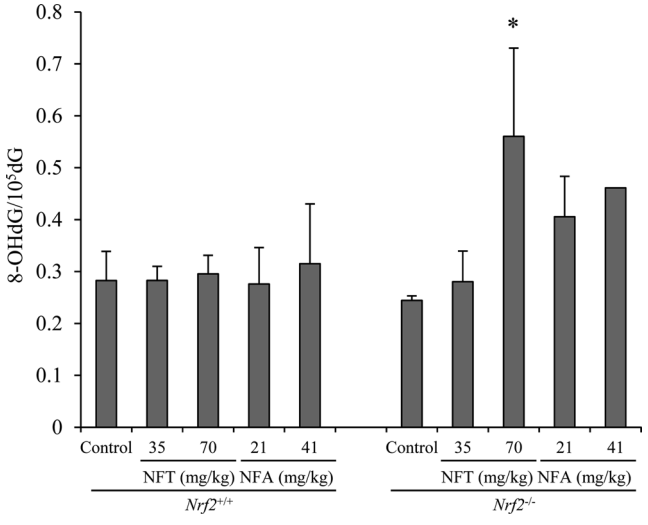

Fig. 4. 8-OHdG levels in the kidneys of *Nrf2*$^{+/+}$ or *Nrf2*$^{-/-}$ *gpt* delta mice treated with NFT or NFA for 13 weeks. Data are presented as means ± SD for 3 mice in the groups treated with other than 41 mg/kg NFA. In the 41 mg/kg NFA group, the data obtained from one mouse are presented. *Significantly different (P<0.05) from levels in the relative control group by Dunnett's test.

to C:G transversions increased in a dose-dependent manner. These changes in spectra of *gpt* mutations were consistent with those observed in NFT-treated *gpt* delta rats[11]. Since guanine bases are susceptible to oxidative modification, the characteristics of the mutation spectra suggest that oxidative stress is involved in NFT-induced genotoxicity. Moreover, 8-OHdG causes G:C to T:A transversions via mispairing with adenine in the course of DNA replication[26, 27]; accordingly, the formation of 8-OHdG may contribute to the G:C to T:A transversions observed in *Nrf2*$^{-/-}$ mice treated with NFT. Furthermore, NFT failed to induce increases in 8-OHdG in *Nrf2*$^{+/+}$ mice, unlike in rats[11], indicating that the sensitivity to oxidative stress is greater in rats than in mice. Considering that NFT does not show carcinogenicity in mice[7], this may explain the difference in NFT carcinogenicity between rats and mice.

Nitro reduction causes oxidative stress in most nitro compounds, including nitrofurans[8–10]. Nitroreductase induces a one-electron reduction of the nitro group, yielding nitro anion radicals, and the chemical instability increases various ROS, such as superoxide anions and hydroxyl radicals, via its electron-donating ability[28]. ROS generation by

Table 2. *Gpt* Mutation Frequencies in Kidneys of *Nrf2*$^{+/+}$ or *Nrf2*$^{-/-}$ *gpt* Delta Mice Treated with NFT or NFA for 13 Weeks

Genotype	Treatment	Animal No.	Cm^R colonies ($\times 10^5$)	6-TG^R and Cm^R colonies	MF ($\times 10^{-5}$)	Mean ± SD
Nrf2$^{+/+}$	Control	W1	25.02	7	0.28	0.46 ± 0.16
		W2	18.00	10	0.56	
		W3	18.09	10	0.55	
		W4	8.24	5	0.61	
		W5	36.99	11	0.30	
	NFT 35 mg/kg	W7	13.95	9	0.65	0.52 ± 0.16
		W8	23.09	7	0.30	
		W9	25.11	15	0.60	
		W10	12.33	5	0.41	
		W11	15.12	10	0.66	
	NFT 70 mg/kg	W13	20.61	4	0.19	0.52 ± 0.23
		W14	22.14	11	0.50	
		W15	17.64	12	0.68	
		W16	7.25	5	0.69	
	NFA 21 mg/kg	W19	22.91	10	0.44	0.33 ± 0.11
		W20	11.61	5	0.43	
		W21	32.49	6	0.18	
		W22	19.80	7	0.35	
		W23	15.44	4	0.26	
	NFA 41 mg/kg	W25	35.15	3	0.09	0.31 ± 0.25
		W26	24.57	6	0.24	
		W27	41.09	3	0.07	
		W28	7.74	4	0.52	
		W29	16.02	10	0.62	
Nrf2$^{-/-}$	Control	Ho1	8.15	4	0.49	0.36 ± 0.16
		Ho2	24.93	8	0.32	
		Ho3	20.43	5	0.24	
		Ho4	11.43	2	0.17	
		Ho5	21.87	12	0.55	
	NFT 35 mg/kg	Ho7	12.15	3	0.25	0.37 ± 0.21
		Ho8	10.26	1	0.10	
		Ho9	28.80	11	0.38	
		Ho10	24.71	16	0.65	
		Ho11	20.34	10	0.49	
	NFT 70 mg/kg	Ho15	10.22	8	0.78	0.85 ± 0.12*
		Ho16	10.22	10	0.98	
		Ho17	19.40	18	0.93	
		Ho18	18.23	13	0.71	
	NFA 21 mg/kg	Ho19	11.48	2	0.17	0.49 ± 0.45
		Ho20	16.56	8	0.48	
		Ho22	18.77	24	1.28	
		Ho23	11.16	3	0.27	
		Ho24	19.67	5	0.25	
	NFA 41 mg/kg	Ho25	16.74	4	0.24	0.46 ± 0.22
		Ho26	11.16	7	0.63	
		Ho28	4.10	1	0.24	
		Ho29	14.99	7	0.47	
		Ho30	18.14	13	0.72	

*$P<0.05$ vs. relative control group. Cm^R, chloramphenicol resistant; 6-TG^R, 6-thioguanine resistant; MF, mutant frequency.

nitroreductase is involved in NFT-induced DNA damage or cytotoxicity in rodent livers and lungs[29, 30]. However, our recent report showed that NFA, a constituent compound of NFT with a nitro group, induced a significant increase in the *gpt* MF, without an elevation in 8-OHdG, in *gpt* delta rats[11]. In the present study, NFA did not increase MFs of the reporter genes in the kidneys of either genotype, despite the tendencies toward increases in 8-OHdG in NFA-treated *Nrf2*$^{-/-}$ mice. These results concerning NFA in rats and mice indicated that it is unlikely that oxidative stress is involved in the genotoxicity of NFA; other factors, such as the direct formation of DNA adducts, as observed for other nitrofurans[31, 32], by NFA, likely to contribute to its genotoxicity.

The results of the present study imply that nitro reduction plays a key role in the genotoxicity of NFT. However, our findings indicate the involvement of oxidative DNA damage in genotoxicity in the kidneys of NFT-treated *Nrf2*$^{-/-}$ mice, but not in the kidneys of NFA-treated *Nrf2*$^{-/-}$ mice. Side chain interactions may affect the generation of oxidative stress by nitro reduction of the nitro group.

Table 3. Mutation Spectra in the Kidneys of *Nrf2*$^{+/+}$ *gpt* Delta Mice Treated with NFT or NFA for 13 Weeks

	Control		NFT 35 mg/kg		NFT 70 mg/kg		NFA 21 mg/kg		NFA 41 mg/kg	
	Number (%)	Specific MFs (10^{-5})	Number (%)	Specific MFs (10^{-5})	Number (%)	Specific MFs (10^{-5})	Number (%)	Specific MFs (10^{-5})	Number (%)	Specific MFs (10^{-5})
Base substitution										
Transversions										
G:C-T:A	8 (26.7)	0.10 ± 0.08	11 (28.9)	0.11 ± 0.09	3 (12.0)	0.07 ± 0.12	5 (18.5)	0.05 ± 0.06	8 (33.3)	0.10 ± 0.10
G:C-C:G	0	0	2 (5.3)	0.02 ± 0.03	3 (12.0)	0.05 ± 0.06	0	0	2 (8.3)	0.03 ± 0.06
A:T-T:A	0	0	2 (5.3)	0.03 ± 0.06	0	0	2 (7.4)	0.02 ± 0.03	1 (4.2)	0.03 ± 0.06
A:T-C:G	0	0	0	0	3 (12.0)	0.05 ± 0.06**	1 (3.7)	0.01 ± 0.02	0	0
Transisions										
G:C-A:T	8 (26.7)	0.09 ± 0.05	13 (34.2)	0.15 ± 0.12	7 (28.0)	0.07 ± 0.10	13 (48.1)	0.13 ± 0.03	4 (16.7)	0.04 ± 0.08
A:T-G:C	5 (16.7)	0.06 ± 0.05	3 (7.9)	0.04 ± 0.06	0	0	0	0	1 (4.2)	0.01 ± 0.02
Deletion										
Single bp	2 (6.7)	0.05 ± 0.11	0	0	3 (12.0)	0.03 ± 0.03	4 (14.8)	0.05 ± 0.03	3 (12.5)	0.03 ± 0.03
Over 2 bp	3 (10)	0.02 ± 0.05	7 (18.4)	0.08 ± 0.05	0	0	1 (3.7)	0.02 ± 0.04	3 (12.5)	0.03 ± 0.03
Insertion	2 (6.7)	0.01 ± 0.02	0	0	3 (12.0)	0.05 ± 0.06	0	0	2 (8.3)	0.02 ± 0.06
Complex	2 (6.7)	0.02 ± 0.05	0	0	3 (12.0)	0.03 ± 0.04	1 (3.7)	0.01 ± 0.02	0	0
Total	30	0.35	38	0.43	25	0.34	27	0.28	24	0.29

**P<0.01, vs. control group. MF, mutant frequency.

Table 4. Mutation Spectra in the Kidneys of *Nrf2*$^{-/-}$ *gpt* Delta Mice Treated with NFT or NFA for 13 Weeks

	Control		NFT 35 mg/kg		NFT 70 mg/kg		NFA 21 mg/kg		NFA 41 mg/kg	
	Number (%)	Specific MFs (10^{-5})	Number (%)	Specific MFs (10^{-5})	Number (%)	Specific MFs (10^{-5})	Number (%)	Specific MFs (10^{-5})	Number (%)	Specific MFs (10^{-5})
Base substitution										
Transversions										
G:C-T:A	4 (13.8)	0.06 ± 0.06	8 (22.2)	0.08 ± 0.06	9 (21.4)	0.15 ± 0.13	7 (31.8)	0.08 ± 0.05	3 (9.4)	0.05 ± 0.08
G:C-C:G	2 (6.9)	0.02 ± 0.03	3 (8.3)	0.02 ± 0.04	7 (16.7)	0.13 ± 0.13	2 (9.1)	0.03 ± 0.04	4 (12.5)	0.06 ± 0.07
A:T-T:A	0	0	0	0	1 (2.4)	0.02 ± 0.05	1 (4.5)	0.01 ± 0.03	2 (6.3)	0.02 ± 0.05
A:T-C:G	2 (6.9)	0.02 ± 0.04	1 (2.8)	0.01 ± 0.02	0	0	0	0	0	0
Transisions										
G:C-A:T	14 (48.3)	0.15 ± 0.08	15 (41.7)	0.14 ± 0.06	13 (31.0)	0.22 ± 0.09	6 (27.3)	0.07 ± 0.05	12 (37.5)	0.14 ± 0.17
A:T-G:C	0	0	2 (5.6)	0.02 ± 0.02	1 (2.4)	0.02 ± 0.05	1 (4.5)	0.01 ± 0.02	1 (3.1)	0.02 ± 0.04
Deletion										
Single bp	6 (20.7)	0.07 ± 0.05	3 (8.3)	0.02 ± 0.03	5 (11.9)	0.09 ± 0.07	2 (9.1)	0.03 ± 0.04	1 (3.1)	0.01 ± 0.03
Over 2 bp	1 (3)	0.01 ± 0.02	2 (5.6)	0.02 ± 0.02	2 (4.8)	0.03 ± 0.05	0	0	4 (12.5)	0.05 ± 0.05
Insertion	0	0	1 (2.8)	0.01 ± 0.02	1 (2.4)	0.02 ± 0.05	1 (4.5)	0.02 ± 0.04	2 (6.3)	0.06 ± 0.11
Complex	0	0	1 (2.8)	0.01 ± 0.02	3 (7.1)	0.06 ± 0.09	2 (9.1)	0.02 ± 0.05	3 (9.4)	0.05 ± 0.08
Total	29	0.32	36	0.33	42	0.75	22	0.28	32	0.46

MF, mutant frequency.

Table 5. Spi⁻ Mutant Frequencies in Kidneys of *Nrf2*$^{+/+}$ or *Nrf2*$^{-/-}$ *gpt* Delta Mice Treated with NFT or NFA for 13 Weeks

Genotype	Treatment	Animal No.	Plaques within XL-1 Blue MRA (× 10^5)	Plaques within XL-1 Blue MRA (P2)	MF (× 10^{-5})	Mean ± SD
Nrf2$^{+/+}$	Control	W1	20.34	4	0.20	0.35 ± 0.34
		W2	18.45	2	0.11	
		W3	11.70	3	0.26	
		W4	4.23	4	0.95	
		W5	33.39	8	0.24	
	NFT 35 mg/kg	W7	22.23	11	0.49	0.50 ± 0.21
		W8	10.35	6	0.58	
		W9	19.71	12	0.61	
		W10	7.29	5	0.69	
		W11	13.95	2	0.14	
	NFT 70 mg/kg	W13	19.35	5	0.26	0.33 ± 0.30
		W14	15.39	12	0.78	
		W15	22.77	4	0.18	
		W16	4.41	2	0.45	
		W17	4.95	0	0.00	
	NFA 21 mg/kg	W19	26.46	7	0.26	0.35 ± 0.06
		W20	10.98	4	0.36	
		W21	25.20	8	0.32	
		W22	16.74	7	0.42	
		W23	10.89	4	0.37	
	NFA 41 mg/kg	W25	36.09	4	0.11	0.34 ± 0.13
		W26	16.74	7	0.42	
		W27	34.56	15	0.43	
		W28	10.44	4	0.38	
		W29	13.32	5	0.38	
Nrf2$^{-/-}$	Control	Ho1	6.39	3	0.47	0.34 ± 0.18
		Ho2	19.62	5	0.25	
		Ho3	14.04	2	0.14	
		Ho4	10.53	6	0.57	
		Ho5	20.34	5	0.25	
	NFT 35 mg/kg	Ho7	13.14	7	0.53	0.43 ± 0.18
		Ho8	10.44	2	0.19	
		Ho9	26.01	7	0.27	
		Ho10	21.78	13	0.60	
		Ho11	21.69	12	0.55	
	NFT 70 mg/kg	Ho15	12.69	7	0.55	0.45 ± 0.09
		Ho16	12.24	5	0.41	
		Ho17	18.54	9	0.49	
		Ho18	19.62	7	0.36	
	NFA 21 mg/kg	Ho19	11.34	0	0.00	0.35 ± 0.27
		Ho20	13.86	5	0.36	
		Ho22	36.72	12	0.33	
		Ho23	14.13	4	0.28	
		Ho24	15.66	12	0.77	
	NFA 41 mg/kg	Ho25	17.64	8	0.45	0.49 ± 0.19
		Ho26	9.27	3	0.32	
		Ho28	3.69	3	0.81	
		Ho29	14.04	7	0.50	
		Ho30	23.58	9	0.38	

MF, mutant frequency.

In conclusion, the results of the present study demonstrated that oxidative stress is involved in NFT-induced genotoxicity in mouse kidneys, consistent with previous results in rats, and that oxidative stress was not involved in the genotoxic mechanism of NFA, a constituent compound of NFT with a nitro group. This might be due to the influence by side chains on the generation of oxidative stress by the nitro reduction of the nitro group. The oxidative stress induced by side chain binding should be considered in the development of new nitrofuran compounds.

Disclosure of Potential Conflicts of Interest: The authors declare that they have no competing interests.

References

1. IARC Working Group on the Evaluation of the Carcinogenic Risk to Humans Furaltadone. In: IARC Monographs on the Evaluation of Carcinogenic Risks to Humans, vol. 7, International Agency for Research on Cancer, Lyon. 161–169. 1974.
2. IARC Working Group on the Evaluation of the Carcinogenic Risk to Humans Furazolidone. In: IARC Monographs on the Evaluation of the Carcinogenic Risk to Humans, vol. 31, International Agency for Research on Cancer, Lyon. 1983.
3. IARC Working Group on the Evaluation of the Carcinogenic Risk to Humans Nitrofural (nitrofurazone). In: IARC Monographs on the Evaluation of the Carcinogenic Risks of Chemicals to Humans, vol. 50, International Agency for Research on Cancer, Lyon. 195–209. 1990.
4. IARC Working Group on the Evaluation of the Carcinogenic Risk to Humans. Nitrofurantoin. In: IARC Monographs on the Evaluation of the Carcinogenic Risks to Humans, vol. 50, International Agency for Research on Cancer, Lyon. 211–231. 1990.
5. Zorzi RR, Jorge SD, Palace-Berl F, Pasqualoto KF, Bortolozzo LS, de Castro Siqueira AM, and Tavares LC. Exploring 5-nitrofuran derivatives against nosocomial pathogens: synthesis, antimicrobial activity and chemometric analysis. Bioorg Med Chem. **22**: 2844–2854. 2014. [Medline] [CrossRef]
6. Fleck LE, North EJ, Lee RE, Mulcahy LR, Casadei G, and Lewis K. A screen for and validation of prodrug antimicrobials. Antimicrob Agents Chemother. **58**: 1410–1419. 2014. [Medline] [CrossRef]
7. National Toxicology Program NTP toxicology and carcinogenesis studies of nitrofurantoin (CAS No. 67–20–9) in F344/N rats and B6C3F1 mice (feed studies). Natl Toxicol Program Tech Rep Ser. **341**: 1–218. 1989. [Medline]
8. Chung MC, Bosquesi PL, and dos Santos JL. A prodrug approach to improve the physico-chemical properties and decrease the genotoxicity of nitro compounds. Curr Pharm Des. **17**: 3515–3526. 2011. [Medline] [CrossRef]
9. Boelsterli UA, Ho HK, Zhou S, and Leow KY. Bioactivation and hepatotoxicity of nitroaromatic drugs. Curr Drug Metab. **7**: 715–727. 2006. [Medline] [CrossRef]
10. Bartel LC, Montalto de Mecca M, and Castro JA. Nitroreductive metabolic activation of some carcinogenic nitro heterocyclic food contaminants in rat mammary tissue cellular fractions. Food Chem Toxicol. **47**: 140–144. 2009. [Medline] [CrossRef]
11. Kijima A, Ishii Y, Takasu S, Matsushita K, Kuroda K, Hibi D, Suzuki Y, Nohmi T, and Umemura T. Chemical structure-related mechanisms underlying in vivo genotoxicity induced by nitrofurantoin and its constituent moieties in gpt delta rats. Toxicology. **331**: 125–135. 2015. [Medline] [CrossRef]
12. Lee JS, and Surh YJ. Nrf2 as a novel molecular target for chemoprevention. Cancer Lett. **224**: 171–184. 2005. [Medline] [CrossRef]
13. Jaiswal AK. Regulation of genes encoding NAD(P)H:quinone oxidoreductases. Free Radic Biol Med. **29**: 254–262. 2000. [Medline] [CrossRef]
14. Yokoo Y, Kijima A, Ishii Y, Takasu S, Tsuchiya T, and Umemura T. Effects of Nrf2 silencing on oxidative stress-associated intestinal carcinogenesis in mice. Cancer Med. **5**: 1228–1238. 2016. [Medline] [CrossRef]
15. Umemura T, Kuroiwa Y, Kitamura Y, Ishii Y, Kanki K, Kodama Y, Itoh K, Yamamoto M, Nishikawa A, and Hirose M. A crucial role of Nrf2 in in vivo defense against oxidative damage by an environmental pollutant, pentachlorophenol. Toxicol Sci. **90**: 111–119. 2006. [Medline] [CrossRef]
16. Tasaki M, Kuroiwa Y, Inoue T, Hibi D, Matsushita K, Kijima A, Maruyama S, Nishikawa A, and Umemura T. Lack of nrf2 results in progression of proliferative lesions to neoplasms induced by long-term exposure to non-genotoxic hepatocarcinogens involving oxidative stress. Exp Toxicol Pathol. **66**: 19–26. 2014. [Medline] [CrossRef]
17. Kitamura Y, Umemura T, Kanki K, Kodama Y, Kitamoto S, Saito K, Itoh K, Yamamoto M, Masegi T, Nishikawa A, and Hirose M. Increased susceptibility to hepatocarcinogenicity of Nrf2-deficient mice exposed to 2-amino-3-methylimidazo[4,5-f]quinoline. Cancer Sci. **98**: 19–24. 2007. [Medline] [CrossRef]
18. Kanki K, Umemura T, Kitamura Y, Ishii Y, Kuroiwa Y, Kodama Y, Itoh K, Yamamoto M, Nishikawa A, and Hirose M. A possible role of nrf2 in prevention of renal oxidative damage by ferric nitrilotriacetate. Toxicol Pathol. **36**: 353–361. 2008. [Medline] [CrossRef]
19. Hu X, Roberts JR, Apopa PL, Kan YW, and Ma Q. Accelerated ovarian failure induced by 4-vinyl cyclohexene diepoxide in Nrf2 null mice. Mol Cell Biol. **26**: 940–954. 2006. [Medline] [CrossRef]
20. Enomoto A, Itoh K, Nagayoshi E, Haruta J, Kimura T, O'Connor T, Harada T, and Yamamoto M. High sensitivity of Nrf2 knockout mice to acetaminophen hepatotoxicity associated with decreased expression of ARE-regulated drug metabolizing enzymes and antioxidant genes. Toxicol Sci. **59**: 169–177. 2001. [Medline] [CrossRef]
21. Nohmi T, Suzuki T, and Masumura K. Recent advances in the protocols of transgenic mouse mutation assays. Mutat Res. **455**: 191–215. 2000. [Medline] [CrossRef]
22. Matsushita K, Ishii Y, Takasu S, Kuroda K, Kijima A, Tsuchiya T, Kawaguchi H, Miyoshi N, Nohmi T, Ogawa K, Nishikawa A, and Umemura T. A medium-term gpt delta rat model as an in vivo system for analysis of renal carcinogenesis and the underlying mode of action. Exp Toxicol Pathol. **67**: 31–39. 2015. [Medline] [CrossRef]
23. Itoh K, Chiba T, Takahashi S, Ishii T, Igarashi K, Katoh Y, Oyake T, Hayashi N, Satoh K, Hatayama I, Yamamoto M, and Nabeshima Y. An Nrf2/small Maf heterodimer mediates the induction of phase II detoxifying enzyme genes through antioxidant response elements. Biochem Biophys Res Commun. **236**: 313–322. 1997. [Medline] [CrossRef]
24. Umemura T, Kai S, Hasegawa R, Kanki K, Kitamura Y, Nishikawa A, and Hirose M. Prevention of dual promoting effects of pentachlorophenol, an environmental pollutant, on diethylnitrosamine-induced hepato- and cholangiocarcinogenesis in mice by green tea infusion. Carcinogenesis. **24**: 1105–1109. 2003. [Medline] [CrossRef]
25. Umemura T, Kanki K, Kuroiwa Y, Ishii Y, Okano K, Nohmi T, Nishikawa A, and Hirose M. In vivo mutagenicity and initiation following oxidative DNA lesion in the kidneys of rats given potassium bromate. Cancer Sci. **97**: 829–835. 2006. [Medline] [CrossRef]
26. Nakabeppu Y. Cellular levels of 8-oxoguanine in either DNA or the nucleotide pool play pivotal roles in carcinogenesis and survival of cancer cells. Int J Mol Sci. **15**:

12543–12557. 2014. [Medline] [CrossRef]
27. Nohmi T, Kim SR, and Yamada M. Modulation of oxidative mutagenesis and carcinogenesis by polymorphic forms of human DNA repair enzymes. Mutat Res. **591**: 60–73. 2005. [Medline] [CrossRef]
28. Wang Y, Gray JP, Mishin V, Heck DE, Laskin DL, and Laskin JD. Role of cytochrome P450 reductase in nitrofurantoin-induced redox cycling and cytotoxicity. Free Radic Biol Med. **44**: 1169–1179. 2008. [Medline] [CrossRef]
29. Rossi L, Silva JM, McGirr LG, and O'Brien PJ. Nitrofurantoin-mediated oxidative stress cytotoxicity in isolated rat hepatocytes. Biochem Pharmacol. **37**: 3109–3117. 1988. [Medline] [CrossRef]
30. Suntres ZE, and Shek PN. Nitrofurantoin-induced pulmonary toxicity. In vivo evidence for oxidative stress-mediated mechanisms. Biochem Pharmacol. **43**: 1127–1135. 1992. [Medline] [CrossRef]
31. Streeter AJ, and Hoener BA. Evidence for the involvement of a nitrenium ion in the covalent binding of nitrofurazone to DNA. Pharm Res. **5**: 434–436. 1988. [Medline] [CrossRef]
32. Touati E, Phillips DH, Quillardet P, and Hofnung M. Determination of target nucleotides involved in 7-methoxy-2-nitro-naphtho[2,1-b]furan (R7000)-DNA adduct formation. Mutagenesis. **8**: 149–154. 1993. [Medline] [CrossRef]